average for 16 scans, and the FD values represent an average of eight scans. The experimental intensities for most masses are within 10% (relative) of the theoretical values. Our experience with FD and FAB is that this result is a close match and strong evidence of the composition.

Conclusions and Final Comments. Both FD and FAB mass spectrometry are viable techniques for the analysis and characterization of a wide variety of organometallic complexes.[18] As with the coordination complexes, the two seem to be complementary in nature; FD, a more gentle technique, provides information on the intact complex cation (or, for neutral complexes, the molecular ion), and FAB reveals aspects of the ligands through fragment ions. It is appropriate to use FAB initially, especially because it is easier to use. If the intact complex must be characterized, FD may then be used.

Schemes I and II permit interpretation of the fragmentation patterns of $[Me(bpy)_2(L)X]^+$ complexes and are based on three concepts: the lability of L; the oxidative-addition reaction of bpy to form carbon-bound (bpy - H) ligand; the reductive elimination of HX. Thermally induced FAB reaction chemistry should provide the basis to predict fragmentation patterns of other organometallic species, especially of low-valent, electron-rich metals.

Acknowledgment. This work was partially supported by National Science Foundation Grant CHE-8210801.

Registry No. $[Os(bpy)_2(\eta^2\text{-}CH{=}CH_2)Cl](PF_6)$, 81831-18-7; $[Os(bpy)_2(\eta^2\text{-}PhCH{=}CH_2)Cl](PF_6)$, 81846-90-4; $[Os(bpy)_2(\eta^2\text{-}CH_3CH_2C{\equiv}CCH_2CH_3)Cl](PF_6)$, 81846-88-0; $[Os(bpy)_2(\eta^2\text{-}PhC{\equiv}CCH_2CH_3)Cl](PF_6)$, 93966-26-8; $[Os(bpy)_2(\eta^2\text{-}CH_3CO_2C{\equiv}CCO_2CH_3)Cl](PF_6)$, 81831-20-1; $[Ru(\eta^6\text{-}C_6H_6)(bpy)Cl](PF_6)$, 76761-93-8; $Ru(\eta^5\text{-}C_5H_5)(bpy)Cl$, 93966-27-9; $[Ru(bpy)_2(CO)Cl](PF_6)$, 79850-20-7; $[Os(bpy)_2(CO)Cl](PF_6)$, 80502-54-1; $[Ru(bpy)_2(CO)O_2CH](PF_6)$, 84117-41-9; $[Os(bpy)_2(CO)O_2CH](PF_6)$, 84117-43-1; $[Os(bpy)_2(CO)O_2CCF_3](PF_6)$, 94062-23-4; $[Ru(bpy)_2(CO)((CH_2)_4CH_3)](PF_6)$, 93966-29-1; $[Ru(bpy)_2(CO)CH_2Ph](PF_6)$, 82482-60-8; $[Ru(bpy)_2(CO)CD_2Ph](PF_6)$, 93966-31-5; $[Os(bpy)_2(CO)CH_2Ph](PF_6)$, 93966-33-7; $[Os(bpy)_2(CO)H](PF_6)$, 84117-35-1.

Contribution from the Chemistry Department, University of Auckland, Auckland, New Zealand, and CSIRO, Division of Materials Science, Catalysis and Surface Science Laboratory, University of Melbourne, Parkville, Victoria, Australia

Electron Spin Resonance Studies of the One-Electron-Reduction Products of Nickel(II) 1,3-Dithio β-Diketonate Complexes

GRAHAM A. BOWMAKER,† PETER D. W. BOYD,*† MARUTA ZVAGULIS,† KINGSLEY J. CAVELL,‡ and ANTHONY F. MASTERS‡

Received February 17, 1984

The ESR spectra of the initial one-electron-reduction products of nickel(II) bis(1,3-dithio β-diketonate), $Ni(SacSac)_2$, have been observed at low temperatures after controlled-potential electrolysis. The spectra are well resolved and at 77 K show anisotropic *g* values, which are intermediate in magnitude between those found in sulfur-containing radical anions and nickel(I) d^9 complexes. In addition hyperfine interaction is observed between the unpaired electron and the four equivalent methyl groups of the SacSac ligand while no coupling is observed to the methine proton. The results are consistent with a ligand-based reduction, the electron entering a ligand p_π molecular orbital with nodes at the 2-carbons. This is in agreement with recently reported INDO calculations of the electronic structure of $Ni(S_2C_3H_3)_2$ and SW-$X\alpha$ calculations reported in this work. In contrast, the one-electron-reduction product of [Ni(dpe)(SacSac)][BPh_4] (dpe = 1,2-bis(diphenylphosphino)ethane) is found to give the unpaired electron in a metal-based molecular orbital as has been found in other mixed-ligand dpe/bidentate sulfur ligand complexes. ESR spectra of the analogous $[Pd(SacSac)_2]^-$ monoanion are less anisotropic but show larger coupling in the perpendicular region of the spectrum to the methyl protons. This is again consistent with a π-type singly occupied molecular orbital (SOMO) similar to that found in the $[Ni(SacSac)_2]^-$ monoanion.

Introduction

Electrochemical methods such as cyclic voltammetry and other controlled-potential techniques allow the ready investigation of the redox properties of transition-metal complexes. An attractive feature of these techniques is that we may view the working electrode as adding or removing electrons to or from the solute molecule, to the lowest unoccupied molecular orbital (LUMO) or from the highest occupied molecular orbital (HOMO). However, the detailed electronic nature of the species produced in the electrochemical process is often less well-known; many such species are highly reactive or difficult to isolate and characterize by conventional chemical and structural methods.

Recent studies[1-3] of the redox chemistry of group 8 nickel(II), palladium(II), and platinum(II) complexes of bidentate sulfur and other ligands combined with electron spin resonance spectroscopy have, in the case of one-electron reduction, given information on the LUMO of the complex. In particular it has been possible to decide in many cases whether the unpaired electron is occupying a molecular orbital primarily localized on the metal atom leading to a d^9 monovalent, M(I), complex[1] or is delocalized over the ligands to give a divalent radical anion complex.[3] Thus, the initial one-electron reduction of both bis(dialkydithiocarbamato)nickel(II), $Ni(S_2CNR_2)_2$,[1] and the bis(maleonitriledithiolato)nickel(II) dianion,[2] $[Ni(S_2C_4N_2)_2]^{2-}$, for example have been found to be metal based, leading to the appropriate nickel(I) complex (Figure 1). The singly occupied molecular orbital (SOMO) of b_{1g} symmetry is principally composed of the nickel d_{xy} orbital ($\alpha^2 = 0.8$ for $[Ni(S_2CNR_2)_2]^-$ and $\alpha^2 = 0.7$-0.8 for $[Ni(S_2C_4N_2)_2]^{3-}$) and the sulfur ligand p_σ orbitals.

The electrochemical properties in acetone/tetraethylammonium perchlorate of the analogous 1,3-dithiol ligand complexes[4] (Figure 2), bis(1,3-dithio β-diketonate)nickel(II), were first reported by Bond, Heath, and Martin.[5] They found that the molecule bis(dithioacetylacetonato)nickel(II), $Ni(SacSac)_2$, underwent an initial reversible one-electron reduction, at mercury electrodes, followed by a further chemical reaction (without ligand loss) to a species that was reoxidizable to the neutral $Ni(SacSac)_2$. Geiger and co-workers[6] investigated this reduction using cyclic voltam-

† University of Auckland.
‡ University of Melbourne.

(1) Bowmaker, G. A.; Boyd, P. D. W.; Campbell, G. K.; Hope, J. M.; Martin, R. L. *Inorg. Chem.* **1982**, *21*, 1152.
(2) Geiger, W. E., Jr.; Allen, C. S.; Mines, T. E.; Senftleber, F. C. *Inorg. Chem.* **1977**, *16*, 2003.
(3) Bowmaker, G. A.; Boyd, P. D. W.; Campbell, G. K. *Inorg. Chem.* **1982**, *21*, 3565.
(4) Lockyer, T. N.; Martin, R. L.; *Prog. Inorg. Chem.* **1980**, *27*, 223.
(5) Bond, A. M.; Heath, G. A.; Martin, R. L. *Inorg. Chem.* **1971**, *10*, 2026.

0020-1669/85/1324-0401$01.50/0

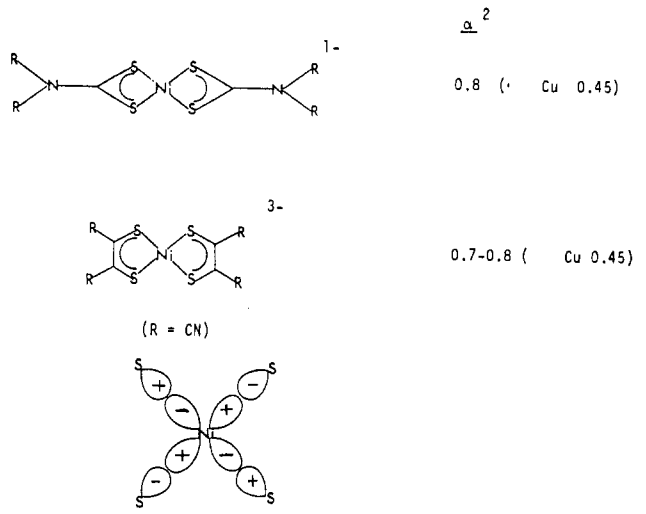

Figure 1. Complexes of nickel(I) with a b_{1g} SOMO.

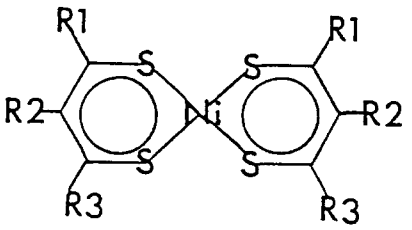

R_1	R_2	R_3	
CH_3	H	CH_3	$Ni(SacSac)_2$
$t\text{-}C_4H_9$	H	$t\text{-}C_4H_9$	$Ni(Bu^tSac\ Bu^tSac)_2$
CH_3	allyl	CH_3	$Ni(CH_2{=}CHCH_2\text{-}SacSac)_2$
CF_3	H	CH_3	$Ni(CF_3\ SacSac)_2$
CH_3	H	Nor*	$Ni(Nor\ SacSac)_2$

*Nor = norbornadienyl

Figure 2. Nickel(II) bis(1,3-dithio β-diketonate).

metry at platinum electrodes in dichloromethane. They found that the monoanion, $[Ni(SacSac)_2]^-$, was stable at moderate scan rates ($i_p^r/i_p^f \sim 1$), but on increasing the concentration of the complex in solution the ratio (i_p^r/i_p^f) decreased, suggesting a further reaction as found by Bond, Heath, and Martin. In an attempt to characterize the initially produced monoanion, attempts were made to measure the ESR spectra of samples of solution taken from a controlled-potential one-electron reduction of $Ni(SacSac)_2$, but no signals were observed. They then proposed the follow-up reaction (Figure 3) to be a dimerization of the monoanion in a similar fashion to that found in 1,2-dithiolate chemistry.[7] It has been proposed from considerations of the large variation of reduction potential with substituent (~1.0 V) and

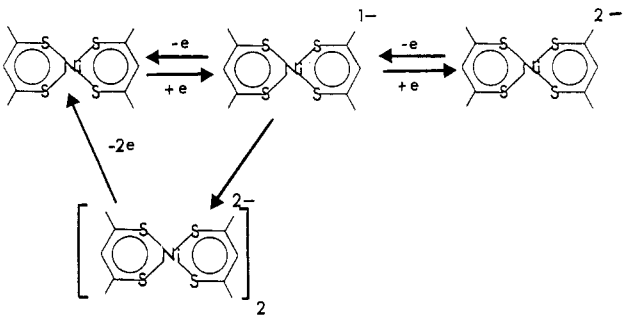

Figure 3. Electrochemical reduction proccesses for $Ni(SacSac)_2$: E_1E_2 vs. E_1CE_R.[6]

the fact that the first reduction potential for the series $Ni(SacSac)_2$, $Pd(SacSac)_2$, and $Pt(SacSac)_2$ was nearly independent of the metal that the SOMO of the monoanion was principally ligand based. More recently the electrochemical properties of nickel, palladium, and platinum bis(1,3-dithio β-diketones) have been reinvestigated by Heath and Leslie[8] using dc and ac polarography and dc cyclic voltammetry. They confirmed the earlier findings[5,6] on the dimerization of the monoanion and found this reaction could be suppressed in complexes with bulkier 1,3-substituents.

We report in this work studies of the ESR spectra of the monoanion produced in the one-electron reduction of various nickel and palladium 1,3-dithio β-diketonate complexes at lower than room temperature and information relating to the spin distribution in these complexes.

Experimental Section

Materials. Complexes $Ni(SacSac)_2$, $Ni(CF_3SacSac)_2$, $Ni(CH_2{=}CHCH_2{-}SacSac)_2$, and $Ni(NorSacSac)_2$ (Nor = norbornene) were prepared by the method described by Barraclough, Martin, and Stewart[10,11] from the appropriate β-diketone. Ni-(*t*-BuSac-*t*-BuSac)$_2$ was prepared by the method of Blejean[12] and purified by vacuum sublimation. All complexes were characterized by proton NMR spectroscopy on a Varian EM360L spectrometer and by microanalysis.

$Ni(CH_2{=}CHCH_2{-}SacSac)_2$. Anal. Calcd for $C_{20}H_{18}S_4Ni$: C, 47.89; H, 5.53; S, 31.96. Found: C, 47.61; H, 5.37; S, 31.7.

$Ni(NorSacSac)_2$. Anal. Calcd for $C_{22}H_{26}S_4Ni$: C, 55.35; H, 5.49; S, 26.90. Found: C, 55.35; H, 5.53; S, 26.4.

Preparation of $Pd(SacSac)_2$. Anhydrous hydrogen chloride gas was passed through 15 mL of anhydrous ethanol at 0 °C for 10 min. $Pd(C_6H_5CN)_2Cl_2$ (0.97 g, 2.5 mmol) was dissolved in the resulting solution followed by acetylacetone (2 mL, 19.4 mmol). Anhydrous hydrogen sulfide gas was passed through the cooled solution for 3 h and the solution left under an H_2S atmosphere at room temperature overnight. The solution was then heated to 60 °C and H_2S passed for a further 2 h. Red crystals were isolated from the reaction mixture. Anal. Calcd for $C_{10}H_{14}PdS_4$: C, 32.6; H, 3.8; S, 34.8. Found: C, 32.7; H, 4.1; S, 34.5.

Preparation of $[Ni(SacSac)(dpe)]BPh_4$. A solution of 1,2-bis(diphenylphosphino)ethane in ether was added dropwise to a solution of $Ni(SacSac)(PBu_3)Cl$[13] in ether in a 1:1 mole ratio. A yellow precipitate formed. This was filtered, washed with ether, and dissolved in methanol. A solution of $NaBPh_4$ in methanol was added slowly with vigorous stirring. A yellow-orange flocculent precipitate separated immediately. On further stirring, the precipitate became crystalline. The yellow-brown solid was separated by filtration, washed with methanol, and dried. Proton NMR indicated the absence of PBu_3 and an approximately 7:1 phenyl:SacSac methyl proton ratio. Anal. Calcd for $C_{55}H_{51}NiS_2P_2B$: C, 72.79; H, 5.66: P, 6.83; S, 7.07; B, 1.19. Found: C, 71.26; H, 5.71; P, 7.5; S, 6.2; B, 0.9.

Electrochemistry. Electrochemical measurements were performed with a platinum working electrode with a PAR 173 potentiostat, PAR 179 digital coulometer with *iR* compensation, and ECG 175 universal programmer.[1] Cyclic voltammograms were measured by a platinum-disk

(6) Bowden, W. L.; Holloway, J. D. L.; Geiger, W. E., Jr. *Inorg. Chem.* **1978**, *17*, 256.
(7) Eisenberg, R. *Prog. Inorg. Chem.* **1970**, *12*, 295.
(8) Heath, G. A.; Leslie, J. H. *J. Chem. Soc., Dalton Trans.* **1983**, 1587.
(9) MacDonald, C. G.; Martin, R. L.; Masters, A. F. *Aust. J. Chem.* **1976**, *29*, 257.
(10) Barraclough, C. G.; Martin, R. L.; Stewart, I. M. *Aust. J. Chem.* **1969**, *22*, 891.
(11) Martin, R. L.; Stewart, I. M. *Nature (London)* **1966**, *210*, 522.
(12) Blejean, C. *Inorg. Nucl. Chem. Lett.* **1971**, *7*, 1011.
(13) Fackler, J.; Masters, A. F. *Inorg. Chim. Acta* **1980**, *39*, 111.

Table I. Coordinates and Radii Used in Calculations[a,b]

atom	x	y	radius I	radius II	α
			$Ni(SacSac)_2$		
Ni	0.0	0.0	2.227	2.62	0.708 96
S	−3.024	2.569	2.311	2.311	0.724 75
C1	−2.290	5.698	1.723	1.600	0.759 28
C2	0.0	6.938	1.687	1.60	0.759 28
H1	−3.916	6.937	1.268	0.95	0.777 25
H2	0.0	8.979	1.269	0.95	0.777 25
OS	0.0	0.0	10.247	9.929	0.740 15
			$[Pd(S_2C_3H_3)_2]^-$		
Pd	0.0	0.0	2.364	2.75	0.701 58
S	3.024	3.096	2.351	2.311	0.724 75
C1	2.294	6.244	1.723	1.60	0.759 28
C2	0.0	7.464	1.687	1.60	0.759 28
H1	3.916	7.464	1.269	1.60	0.777 25
H2	0.0	9.505	1.269	1.60	0.777 25
OS	0.0	0.0	10.774	10.455	0.739 00

[a] Atomic units. [b] $z = 0.0$.

electrode, platinum counterelectrode, and Ag–AgCl (0.1 M LiCl in acetone) reference electrode separated from the voltammetric cell by a 0.1 M LiCl in acetone salt bridge. Measurements were carried out in dichloromethane with 0.1 M $(C_4H_9)_4NClO_4$ supporting electrolyte. The reduction potentials for each of the complexes were referenced to the ferrocene/ferrocenium couple taken as 0.46 V relative to the Ag–AgCl electrode.[1]

Electron Spin Resonance Spectra. X-Band electron spin resonances (ESR) spectra were recorded on a Varian E4 spectrometer. Controlled-potential electrolyses were performed at a platinum-foil electrode in a quartz ESR cell described previously[1] using the following procedure. The ESR cell was placed in a large Schlenk tube that was evacuated and back-filled with dry oxygen-free nitrogen several times. The sample solution of 0.5 M $(C_4H_9)_4NClO_4$ and approximately 0.005 M complex in dichloromethane was degassed by several freeze–thaw cycles in a second Schlenk tube and transferred by syringe to the ESR cell. Electrodes were then inserted into the cell while in the Schlenk tube, under a nitrogen flow, and the top was sealed with Teflon tape. The radical anions of the nickel complexes were then generated by electrolysis, with use of a three-electrode configuration, at potentials slightly greater than the measured reduction potential of the complex. Solution ESR spectra appeared within a few minutes, the signals diminishing with time after the cessation of electrolysis. This diminution could be slowed by performing the electrolyses at lower temperatures, −40 °C, or using more dilute solutions of the complex to inhibit the following dimerization reaction of the radical anion. Frozen-solution spectra were obtained at −160 °C by rapid freezing of the electrolyzed sample. Generally it was found that concentrations of the sample in the range 0.002–0.005 M gave optimum signals in the frozen solution. In the case of the $[Ni(SacSac)(dpe)]^+$ complexes the initially produced solution spectrum was found to be quite stable as expected from electrochemical studies.

Computational Methods. All calculations were performed by using a standard version[14,15] of the SCF–MS–Xα programs on the Auckland University IBM4341 computer. Two sets of calculations were performed with differing radii of the atomic spheres (Table I). Set I was chosen by the criterion of Norman[16] following a superposition of atomic charge densities by the value enclosing an atomic number of electrons on each atom. These were then scaled to give a moderate overlap of atomic spheres (scale factor 0.88).[17] Set II was chosen in a more ad hoc manner from values reported in the literature for first-row transition metals and carbon hydrogen, and nitrogen.[18] The α values used in the calculations were those reported by Schwarz[19] while for the intersphere and outer-sphere values of α were taken as a valence electron number average of these atomic values. The partial wave expansion in each calculation was limited to $l = 4$ for the outer sphere, $l = 2$ for the central transition-metal atom, and $l = 1$ for the rest of the atoms in the molecule except hydrogen ($l = 0$). A Watson sphere of charge 1+ was used for $[Ni(S_2C_3H_3)_2]^-$ and $[Pd(S_2C_3H_3)_2]^-$ with radius equal to the outer-sphere radius. The SCF–Xα–multiple scattering calculation was continued until the relative change in potential at all points was less than 10^{-4}. Charge distributions were calculated according to the methods of Case, Cook, and Karplus.[20,21] The **g** tensors were calculated from the converged Xα wave functions and energies.[18,22]

Table II. Cyclic Voltammetry Parameters for One-Electron-Reduction Reactions of Nickel(II) 1,3-Dithio β-Diketonate Complexes in Dichloromethane at Room Temperature

	E_0',[a] V	ΔE_{pp},[b] mV
$Ni(SacSac)_2$	−1.17	100
$Ni(t\text{-BuSac-}t\text{-BuSac})_2$	−1.26	85
$Ni(CH_2{=}CHCH_2SacSac)_2$	−1.30	120
$Ni(CF_3SacSac)_2$	−0.70	110
$Ni(NorSacSac)_2$	−1.21	90
$[Ni(SacSac)(dpe)]^+$	−0.96	95
$[Ni(t\text{-BuSac-}t\text{-BuSac})dpe]^+$	−0.99	140
$Pd(SacSac)_2$	−1.16	100

[a] Referenced to the ferrocene/ferrocenium couple at 0.46 V relative to Ag–AgCl in 0.1 M LiCl.[1] [b] Scan rate 20 mV/s.

Table III. ESR Parameters for One-Electron-Reduction Products of Bis(1,3-dithio β-diketonato)nickel(II) and Related Complexes in Dichloromethane Solvent

	g_{iso}	g_1	g_2 (=g_3)	ref
$[Ni(SacSac)_2]^-$	2.063	2.088	2.019	this work
$[Ni(t\text{-BuSac-}t\text{-BuSac})_2]^-$	2.061	2.080	2.015	this work
$[Ni(CH_2{=}CHCH_2SacSac)_2]^-$	2.025	2.100	2.013	this work
$[Ni(CF_3SacSac)_2]^-$	2.035	2.068	2.014	this work
$[Ni(NorSacSac)_2]^-$	2.060	2.091	2.021	this work
$[Pd(SacSac)_2]^-$	2.023	2.045	2.008	this work
$[Ni(Bu_2NCS_2)_2]^-$	2.131[a]	2.27	2.062	1
$[Ni(mnt)_2]^{3-}$	2.116[a]	2.205	2.071[b]	2

[a] Average of anisotropic values. [b] Averaged g_2 and g_3 values.

Results and Discussion

Electrochemistry. The reduction potentials of a variety of nickel(II) bis(1,3-dithio β-diketones) have been reported.[5,6,23] The potentials are very sensitive to substituents in the 1- and 3-positions of the ring varying from −0.362 V for $Ni(CF_3SacSac)_2$ to −1.345 V for $Ni(PyrrSacSac)_2$,[24] the potential being least negative for the electron-withdrawing substituent and most negative for $-NR_2$ groups. The work of Geiger and co-workers has produced evidence that upon reduction of $Ni(SacSac)_2$ a following dimerization reaction occurs[6] while for $Ni(t\text{-BuSac-}t\text{-BuSac})_2$[8,25] this rapid rearrangement is suppressed due to the steric bulk of the *tert*-butyl substituents. The cyclic voltammograms of complexes studied here have been measured in dichloromethane at platinum-disk working electrode. All voltammograms showed a decreasing ratio of peak currents with decreasing scan rate, the rate of decrease depending on substituent. Estimated potentials relative to the ferrocene/ferrocenium couple are given in Table II.

The electrochemistry of $Pd(SacSac)_2$[5,8] has shown that the monoanion reacts at a faster rate than the $[Ni(SacSac)_2]^-$, leading to comparable amounts of the monoanion and dimer in solution. Cooling to −50 °C suppresses this dimerization.[8] Our dc cyclic voltammetric and ESR measurements support this observation.

Cyclic voltammograms of $[Ni(dpe)(SacSac)][PF_6]$ and the complex $[Ni(dpe)(t\text{-BuSac-}t\text{-BuSac})]^+$ formed in situ by addition of dpe to $Ni(t\text{-BuSac-}t\text{-BuSac})_2$ were highly reversible. The reductions both occurred at less negative potentials than the

(14) Johnson, K. H. *Adv. Quantum. Chem.* **1973**, *7*, 143.
(15) Slater, J. C.; Johnson, K. H. *Phys. Rev. B: Solid State* **1972**, *B5*, 844.
(16) Norman, J. G., Jr. *J. Chem. Phys.* **1974**, *61*, 4630.
(17) Norman, J. G., Jr. *Mol. Phys.* **1976**, *31*, 1191.
(18) Case, D. A.; Karplus, M. *J. Am. Chem. Soc.* **1977**, *99*, 6182. Sontum, S. F.; Case, D. A. *J. Phys. Chem.* **1982**, *86*, 1596.
(19) Schwarz, K. *Phys. Rev. B: Solid State* **1971**, *B5*, 2466.
(20) Case, D. A.; Karplus, M. *Chem. Phys. Lett.* **1976**, *39*, 33.
(21) Case, D. A.; Cook, M.; Karplus, J. *J. Chem. Phys.* **1980**, *73*, 3294.
(22) Sunil, K. K.; Harrison, J. F.; Rogers, M. T. *J. Chem. Phys.* **1982**, *76*, 3078.
(23) Lockyer, T. N.; Martin, R. L. *Prog. Inorg. Chem.* **1980**, *27*, 223.
(24) Hendrickson, A. R.; Hope, J. M.; Martin, R. L. *Inorg. Chem.* **1976**, *15*, 1118.
(25) Bond, A. M.; Martin, R. L.; Masters, A. F. *J. Electroanal. Chem. Interfacial Electrochem.* **1976**, *72*, 187.

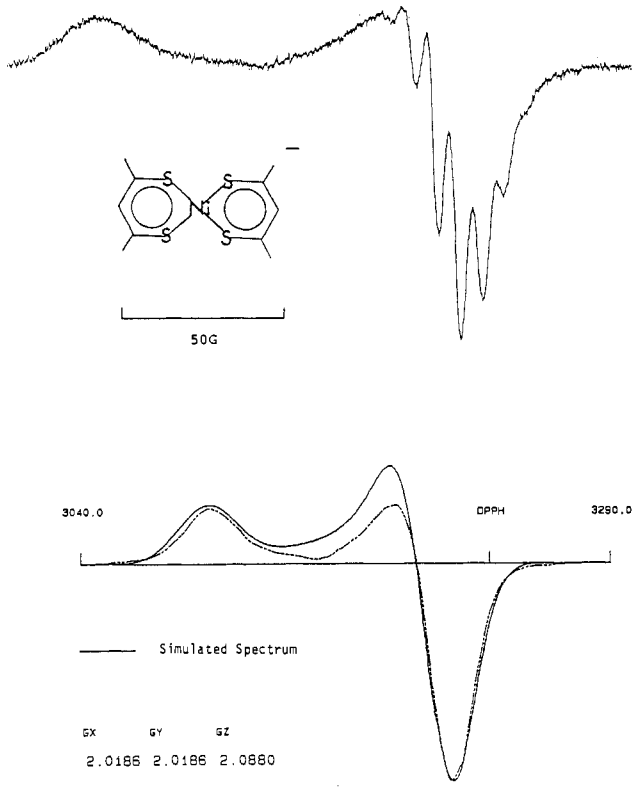

Figure 4. X-Band frozen dichloromethane solution spectrum, −160 °C, of $[Ni(SacSac)_2]^-$ at 9.06 GHz (top) and simulated spectrum (bottom).

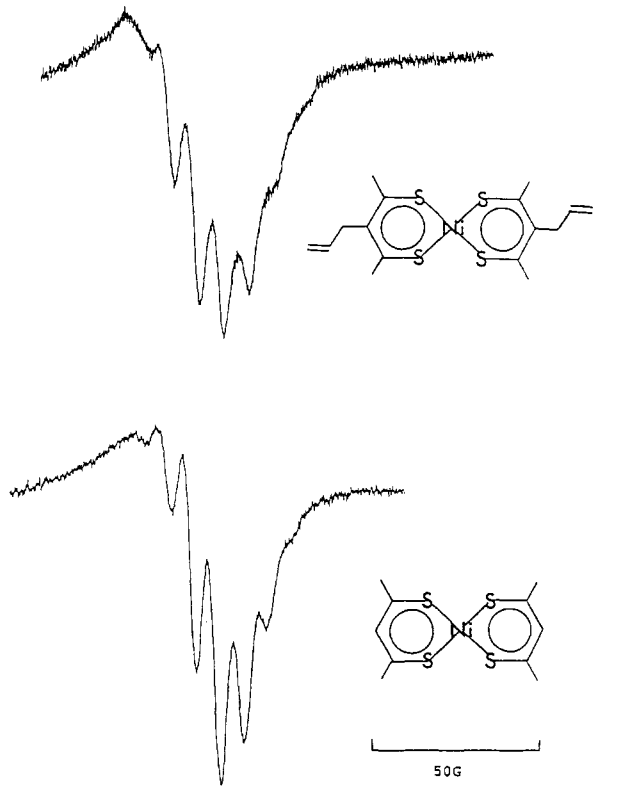

Figure 5. X-Band ESR spectrum of frozen CH_2Cl_2 solution of $[Ni(SacSac)_2]^-$ and $[Ni(CH_2{=}CHCH_2SacSac)_2]^-$ in the perpendicular region.

corresponding bis(dithio β-diketonate) (Table II).

ESR Spectra of the Ni(SacSac)$_2$ Monanion. Electrolysis of dichloromethane solutions of $Ni(SacSac)_2$ at potentials slightly more negative than the first reduction potential of the complex in an in situ ESR electrolysis cell gave ESR-active solutions. At room temperature a single line at $g = 2.042$ was observed with no resolved hyperfine structure. A weak frozen-solution spectrum was also observed from the sample electrolyzed at room temperature. Stronger frozen-solution spectra could be obtained by performing the electrolysis at lower temperatures, ca. −40 to −60 °C (thus slowing the follow-up reaction of the monoanion), before freezing to liquid-nitrogen temperatures. This is consistent with the ESR-active monoanion $[Ni(SacSac)_2]^-$ dimerizing to give an ESR-inactive coupled system.

The ESR spectrum of a frozen solution of $[Ni(SacSac)_2]^-$ (Table III; Figure 4) was anisotropic with axial or near-axial symmetry ($g_\parallel = 2.088$, $g_\perp = 2.019$) and was reproducible from several independently prepared samples of $Ni(SacSac)_2$. A feature of interest in the perpendicular region of the spectrum was a series of seven to nine lines split by 6.8 (±0.3) G. These appear to be due to coupling of the unpaired electron to the protons of the four equivalent methyl groups of the SacSac ligands. Such a splitting pattern would lead to 13 lines in the intensity ratio 1:12:66:220:495:792:924:792:495:220:66:12:1. The weaker outer lines would not be resolved in this spectrum. There appears to be no resolvable coupling to the central SacSac protons in the 3-position. This is evidenced by comparison of the perpendicular region spectra of $[Ni(SacSac)_2]^-$ and $[Ni(CH_2{=}CHCH_2SacSac)_2]^-$, which are identical (Figure 5) and the complete absence of hyperfine splitting in the reduced complex $[Ni(t\text{-BuSac-}t\text{-BuSac})_2]^-$ (Figure 6).

The spin Hamiltonian g value derived by simulation of the ESR spectra have magnitudes and anisotropies less than expected for nickel(I) complexes[11] but slightly larger than that observed in sulfur-containing radical anions.[26] The relatively large coupling of the unpaired electron to the methyl protons in $Ni(SacSac)_2^-$

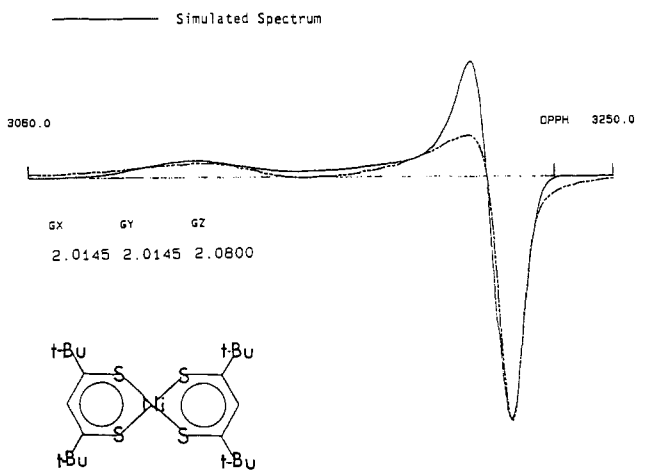

Figure 6. X-Band ESR spectrum of frozen CH_2Cl_2 solution of $[Ni(t\text{-BuSac-}t\text{-BuSac})_2]^-$ at 9.06 GHz.

supports the view that the unpaired electron is delocalized around the $SacSac^-$ chelate ring or at least to the sulfur and adjacent carbon atoms. Recent INDO calculations of the electronic structure of the neutral complex $Ni(S_2C_3H_3)_2$ have been reported by Loew and co-workers.[27] This calculation provided a molecular orbital energy scheme in agreement with electronic spectral properties of the molecule. The lowest unoccupied molecular orbitals calculated for the complex are a nearly degenerate pair of ligand π orbitals of a_u and b_{3g} symmetry. These orbitals provide a basis for the ligand-based singly occupied molecular orbital of $[Ni(S_2C_3H_3)_2]$. The evidence from the ESR spectra of the monoanion then suggests that the LUMO of $Ni(SacSac)_2$ is predominantly ligand based; however the anisotropy of the g tensor

(26) Gilbert, B. D.; Hodgeman, D. K. C.; Norman, R. O. C. *J. Chem. Soc. Perkin Trans. 2* **1973**, 1748.

(27) Herman, Z. S.; Kirchner, R. F.; Loew, G. H.; Mueller-Westerhoff, U. T.; Nazzal, A.; Zerner, M. C. *Inorg. Chem.* **1982**, *21*, 46. The coordinate system used in our work differs from the one used in this reference in that the x and y axes are interchanged.

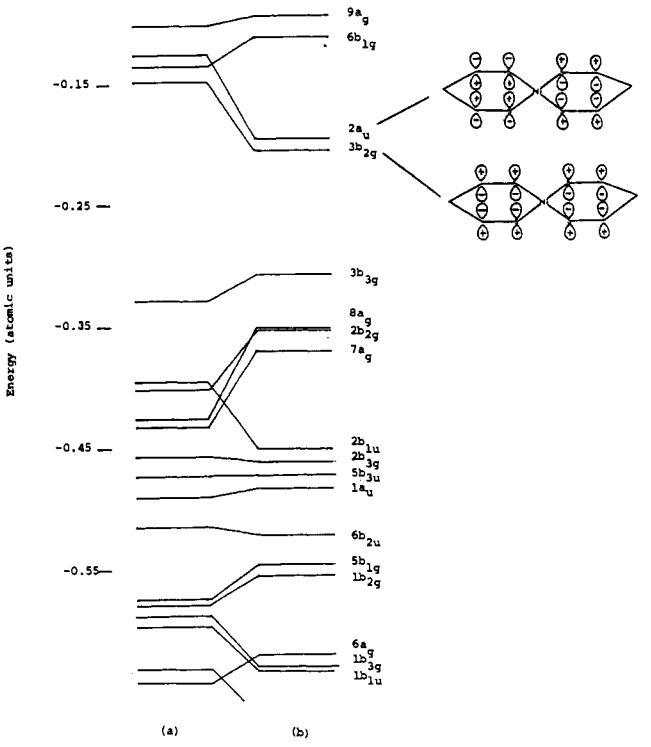

Figure 7. SW-Xα orbital energies for $[Ni(S_2C_3H_3)_2]^-$: (a) calculation I; (b) calculation II.

is larger than would be expected for an organosulfur radical anion.

Electronic Structure of the Ni(SacSac)$_2$ Monoanion. An investigation was made of the nature of the singly occupied molecular orbital and the origin of the **g** tensor anisotropy of the Ni(SacSac)$_2$ monoanion, using SW-Xα calculations on the complex $[Ni(S_2C_3H_3)]^-$. Two sets of atomic sphere radii were used in these calculations (Table I). Set I was chosen by using the Norman procedure[16] and set II chosen by using radii for carbon, hydrogen, and nickel suggested by Case.[18] Calculations using both sets of radii led to the same electronic ground state of the monanion (verified by transition-state calculations with other low-lying levels), namely a singly occupied $3b_{2g}$ level (Table IV; Figure 7). However, as has been reported in other studies of this type on the effect of sphere radii, the use of radii chosen by using the Norman criterion (set I) leads to a significant lowering in energy of the occupied nickel d levels with respect to the ligand levels. Further, the character of the molecular orbitals is changed in some cases quite significantly. For the $3b_{2g}$ SOMO the populations vary from 0.024 Ni (d_{xz}) + 0.035 S (p_z) + 0.208 C (p_z) for set I to 0.131 Ni (d_{xz}) + 0.063 S (p_z) + 0.151 C (p_z) for set II, i.e. the population of the Ni (d_{xz}) orbital changes by a factor of 6.

The relative ordering of the levels for calculation II agrees well with that found in the INDO calculations,[27] with the highest doubly occupied orbital, $3b_{3g}$, being principally a nickel d_{xz} orbital. The energies of the INDO scheme are not strictly comparable to the Xα energies;[18] however, the populations of the SOMO derived from the Xα calculation are in reasonable agreement with the LUMO from the INDO calculation (C, 0.131 vs. 0.130; S, 0.063 vs. 0.036). Both calculations indicate that an electron in the $3b_{2g}$ orbital is delocalized over the sulfur and 1,3-carbon atoms and to some extent the central nickel atom. In fact the highest population of electron density is found on the 1,3-carbon atoms of the SacSac ligand in good qualitative agreement with the observed coupling to methyl group protons attached at this position.

Qualitatively the calculation using radii from set II appears best to explain the observed anisotropies in the **g** tensor of the reduced nickel dithio diketonates where $g_\parallel$ range from 2.1 to 2.07 and $g_\perp$ range from 2.01 to 2.02. The principal values of the **g** tensor for the $3b_{2g}$ SOMO have been evaluated by using perturbation theory[28] including contributions from the nickel d and sulfur p orbitals.[20-22]

Table IV. SW-Xα Orbital Energies and Populations for the $[Ni(S_2C_3H_3)_2]^-$ $3b_{2g}$ SOMO[a]

orbital	energy[b]	populations[d]
$6b_{1g}$	−0.1578	0.657 Ni (d) + 0.007 S (s) + 0.072 S (p)
$2a_u$	−0.2466	0.086 S (p) + 0.164 Cl (p)
$3b_{2g}$[c]	−0.2562	0.131 Ni (d) + 0.063 S (p) + 0.154 Cl (p)
$3b_{3g}$	−0.3571	0.557 Ni (d) + 0.087 S (p) + 0.048 C2 (p)
$8a_g$	−0.4048	0.914 Ni (d) + 0.009 S (p)
$2b_{2g}$	−0.4053	0.705 Ni (d) + 0.008 S (p) + 0.066 Cl (p)
$7a_g$	−0.4208	0.108 Ni (s) + 0.878 Ni (d)
$2b_{1u}$	−0.5022	0.069 Ni (p) + 0.147 S (p) + 0.018 Cl (p) + 0.136 C2 (p)
$2b_{3g}$	−0.5030	0.435 Ni (d) + 0.088 S (p) + 0.012 Cl (p) + 0.084 C2 (p)
$5b_{3u}$	−0.5231	0.155 Ni (d) + 0.195 S (p)
$1a_u$	−0.5332	0.169 S (p) + 0.081 Cl (p)
$6b_{2u}$	−0.5711	0.186 Ni (p) + 0.189 S (p)
$5b_{1g}$	−0.5980	0.282 Ni (d) + 0.015 S (s) + 0.145 S (p)
$1b_{2g}$	−0.6044	0.207 Ni (d) + 0.162 S (p) + 0.036 C (p)
$6a_g$	−0.6711	0.142 Ni (s) + 0.107 Ni (d) + 0.011 S (s) + 0.164 S (p)

[a] Radii set II. [b] Rydberg units. [c] Highest occupied molecular orbital. [d] Populations less than 0.005 omitted.

$$g_x = g_e + \sum_{b_{1g}} \frac{g_e[c_1 d_1 \zeta_d^{Ni} + 4c_2 d_2 \zeta_p^{S}][c_1 d_1 + 4c_2 d_2]}{E(3b_{2g}) - E(b_{1g})}$$

$$g_y = g_e + \sum_{a_g}[g_e[c_1 e_1 \zeta_d^{Ni} - 3^{1/2} c_1 e_2 \zeta_d^{Ni} + 4c_2 e_3 \zeta_p^{S}] \times [c_1 e_1 - 3^{1/2} c_1 e_2 + 4c_2 e_3]]/[E(b_{1g}) - E(a_g)]$$

$$g_z = g_e + \sum_{b_{3g}} \frac{g_e c_1^2 f_1^2 \zeta_d^{Ni}}{E(3b_{2g}) - E(b_{3g})} \quad (1)$$

where $g_e = 2.0023$

$$\psi_{3b_{2g}} = c_1 \phi_{d_{xz}}{}^{Ni} + c_2 \phi_{p_z}{}^{S} + \ldots$$

$$\psi_{b_{1g}} = d_1 \phi_{d_{xy}}{}^{Ni} + d_2 \phi_{p_y}{}^{S} + \ldots$$

$$\psi_{a_g} = e_1 \phi_{d_{x^2-y^2}}{}^{Ni} + e_2 \phi_{d_{z^2}}{}^{Ni} + e_3 \phi_{p_x}{}^{S} + \ldots$$

and

$$\psi_{b_{3g}} = f_1 \phi_{d_{yz}}{}^{Ni} + \ldots$$

The anisotropy of the **g** tensor observed experimentally is larger than can be accounted for in sulfur-containing radical anions and must involve contributions from the nickel atom d levels. Calculation of the **g** tensor using (1) for results from calculation I leads to nearly isotropic values while for calculation II anisotropies approaching those found experimentally are calculated ($g_x = 2.005$, $g_y = 2.039$, $g_z = 2.015$; $\zeta_d^{Ni} = 620$ cm^{-1}, $\zeta_p^{S} = 328$ cm^{-1}). The largest principal g value is calculated to lie along the y axis of the molecule, which passes through the methine carbon atoms and the central nickel atom. Close agreement would not be expected from such calculations as the anisotropies are very sensitively related to the nickel d-orbital content of the $3b_{2g}$ orbital and the relative energies of the $3b_{2g}$ to the b_{1g} (x), a_g (y), and b_{3g} (z) orbitals. The origin of the **g** tensor anisotropy, however, arises mainly from the metal content of the SOMO. In the case of the g_y value the principal contribution to the anisotropy arises by mixing with the metal-based $8a_g$ and $7a_g$ levels.

ESR Spectra. [Ni(dpe)(SacSac)]^0. The ESR spectrum of the one-electron-reduction product of $[Ni(dpe)(SacSac)]^+$ in dichloromethane solution at room temperature consists of three lines due to coupling of the unpaired electron to two equivalent

(28) Abragam A.; Bleaney, B. "Electron Paramagnetic Resonance of Transition Ions"; Clarendon Press: Oxford, 1970.
(29) The summations involved in the **g** tensor calculations were limited to occupied orbitals only.

Table V. ESR Parameters for One-Electron-Reduction Products of Mixed-Ligand Nickel(II) Complexes (Parameters Defined in Figure 8) in Dichloromethane Solvent

	g	g_1	g_2	g_3	a^a	$A_1{}^a$	$A_2{}^a$	$A_3{}^a$	ref
$Ni(S_2CNEt_2)(dpe)$	2.093	2.186	2.043	2.035	83	79	81	92	1
$[Ni(S_2C_2(CN)_2)(dpe)]^-$	2.079	2.161	2.043	2.036	104	92	103	112	3
Ni(SacSac)(dpe)	2.076	2.144	2.044	2.038	98	93	103	102	this work
Ni(*t*-BuSac-*t*-BuSac)(dpe)	2.082	2.138	2.043	2.043		89	104	104	this work

[a] Units: 10^{-4} cm^{-1}.

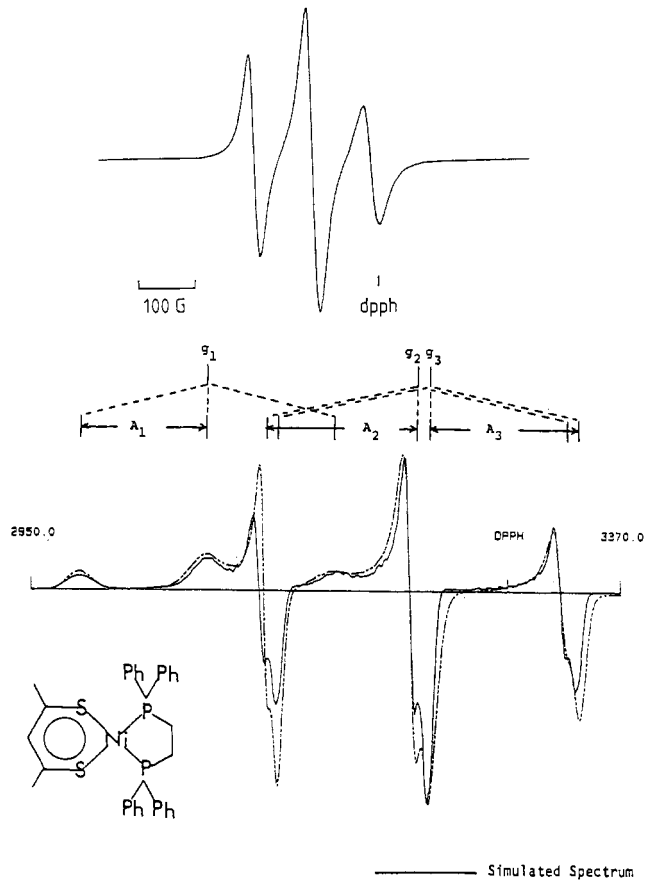

Figure 8. X-Band ESR spectrum of CH_2Cl_2 solution of Ni(SacSac)dpe: (top) −60 °C solution spectrum at 9.25 GHz; (bottom) −160 °C frozen solution spectrum at 9.22 GHz.

phosphorus atoms (Figure 8). The frozen-solution spectrum (Figure 8) is a very well-resolved signal similar to that found for the analogous reduced mixed-ligand complexes $[Ni(dpe)(S_2CNR_2)]^0$ and $[Ni(dpe)(S_2C_4N_2)]^-$. The spectrum again indicates coupling of the single electron to two equivalent phosphorus atoms and anisotropic **g** and hyperfine interaction tensors. A similar but less well-resolved frozen-solution spectrum has been found for the one-electron-reduction product of $[Ni(t\text{-BuSac-}t\text{-BuSac})(dpe)]^+$ (Figure 9).

The parameters g_1, g_2, and g_3 and A_1, A_2, and A_3 were measured from the frozen-solution spectra as shown in Figure 8 and are listed in Table V. As described previously for the related complexes in Table V, A_2 and A_3 are not the principal components of the ^{31}P hyperfine coupling tensor, since the principal axes of the ^{31}P tensor are not expected to coincide with the principal axes of the **g** tensor. The observed splittings A_2 and A_3 depend on the principal components $A_{x'}$ and $A_{y'}$ of the phosphorus hyperfine tensor, and the P–Ni–P angle α.[1,3] As can be seen in Figure 8, reasonable simulations of the observed spectra can be obtained for values of α around 90°, but only if the ^{31}P tensor is made significantly nonaxial ($A_{y'} \neq A_{x'}$). In order to simulate the spectra with axial ^{31}P hyperfine tensors, values of α considerably less than 90° are required. This is similar to the situation encountered previously for related complexes involving the dpe ligand.[3]

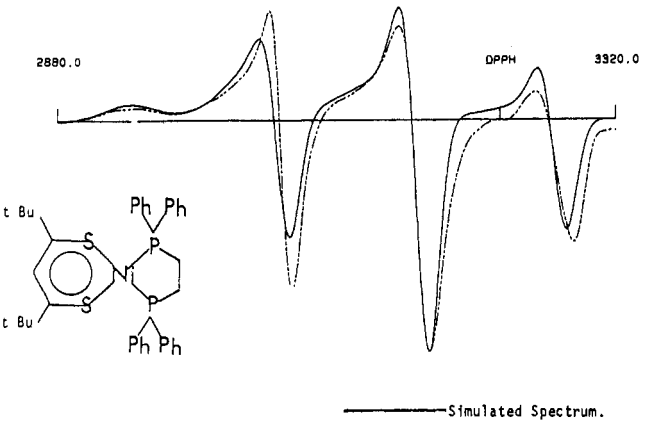

Figure 9. X-Band ESR spectrum of frozen CH_2Cl_2 solution of $[Ni(t\text{-BuSac-}t\text{-BuSac})(dpe)]$ at 9.05 GHz.

The corresponding coupling constants for the mnt and SacSac compounds in Table V are similar in magnitude. It can therefore be concluded that the amount of unpaired spin density in the phosphorus orbitals that these represent is similar for these complexes. This was previously found to be about 0.1 e, residing in the sp^3 donor orbital of the phosphorus atom.[3]

The *g* values for the complexes in Table V are of comparable magnitude, suggesting a similar degree of localization of the unpaired electron on the Ni atom. We have previously shown that the unpaired electron is 70–75% localized on the Ni atom in the dithiocarbamate and maleonitriledithiolate complexes, so that these are properly regarded as nickel(I) species.

The similarity in *g* values for these and the 1,3-dithio diketonate complexes of the present study suggests that these, too, should be regarded as nickel(I) species. If this is correct, there should be an *increase* in the *g* values from the $[Ni(SacSac)_2]^-$ species (where the unpaired electron resides mainly on the ligand) to the Ni(dpe)(SacSac) species, and this is observed experimentally. It should be noted that this contrasts with the situation for the corresponding dithiocarbamate or malenonitriledithiolate complexes where, for example, the *g* values *decrease* from $[Ni(S_2CNR_2)_2]^-$ to $Ni(dpe)(S_2CNR_2)$. This is because, in both of these complexes, the unpaired electron resides mainly on the metal, and the bidentate phosphine ligand allows greater delocalization of spin density (through stronger covalent bonding) than the bidentate sulfur ligand. Thus, the reversal of the previously observed trend in *g* values on replacing a sulfur ligand by a phosphorus ligand in the case of the 1,3-dithio diketone compounds is further evidence for the ligand-centered nature of the reduction of the $Ni(SacSac)_2$ complexes.

The different nature of the SOMO in $[Ni(SacSac)_2]^-$ and Ni(dpe)(SacSac) is further evidenced by the absence of methyl proton hyperfine coupling in the spectrum of the latter compound. The lines in the frozen-solution spectrum of this compound are narrow enough to allow resolution of coupling of the magnitude observed in the perpendicular region of the frozen-solution spectrum of $[Ni(SacSac)_2]^-$ (ca. 7 G) if this had been present.

The $Pd(SacSac)_2$ Monoanion. Electrolysis of dichloromethane solutions of $Pd(SacSac)_2$ in the in situ ESR electrolysis cell at −60 °C gave a solution with a single ESR line at $g = 2.023$. The spectrum obtained on freezing this solution is shown in Figure 10, and the *g* values are given in Table III. The spectrum is axial

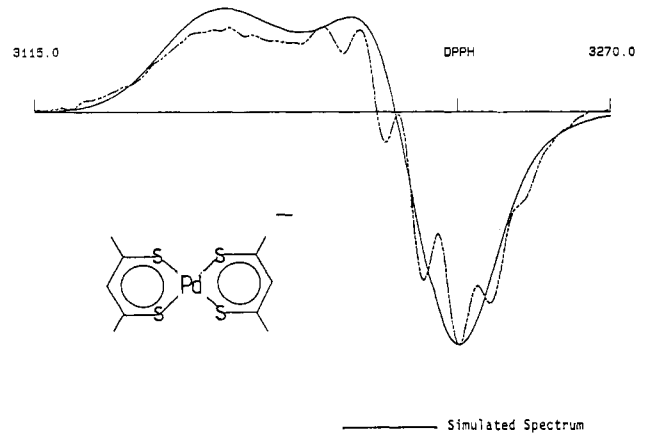

Figure 10. X-Band frozen CH_2Cl_2 solution spectrum, −160 °C, of $[Pd(SacSac)_2]^-$ at 9.06 GHz.

or near-axial, with a smaller degree of anisotropy than in the corresponding nickel species. A hyperfine splitting pattern similar to that observed in the nickel species is clearly resolved in the perpendicular region. The coupling constant is 10 (±0.1) G and is assigned to coupling of the unpaired electron to the methyl groups of the SacSac ligands. This coupling is of the same magnitude as, but slightly larger than, that of the corresponding Ni complex. The spectrum is assigned to the $[Pd(SacSac)_2]^-$ anion, which has been postulated in previous electrochemical studies as the first reduction product of $Pd(SacSac)_2$. In these studies it has been shown that the follow-up reaction of the monoanion to give a dimer is more rapid for the Pd complex than for the Ni complex but is slowed by cooling to −50 °C. This agrees with our observation that the spectrum of the Pd species is more difficult to obtain and is generally of lower intensity than that of the Ni species produced under similar conditions. The similarity in the magnitudes of the proton hyperfine coupling constants for the Ni and Pd species suggests that the same type of SOMO is involved, namely a delocalized ligand π orbital. The fact that the proton hyperfine coupling constant in the Pd complex is greater than that of the Ni complex suggests that the unpaired spin density is greater on the C backbone of the SacSac ligand in the Pd complex.

Electronic Structure of the $Pd(SacSac)_2$ Monoanion. SW-Xα calculations of the electronic structure of the model complex $[Pd(S_2C_3H_3)_2]^-$ were performed with radii described previously (Table I). The ground state of the complex was found in this case to depend on the choice of atomic sphere radius; for set I the singly occupied level was found to be one with the unpaired electron in a "metal-based" $6b_{1g}$ (Ni d_{xy}) orbital (verified by transition-state calculations involving the next lowest lying level) while for set II the singly occupied level was found to be similar to that found in the $Ni(SacSac)_2$ monoanion, $3b_{2g}$ (Figure 11, Table VI).

The range of g value anisotropy ($g_\parallel = 2.045$, $g_\perp = 2.023$) is less than that found for the analogous nickel system even though the spin–orbit coupling of palladium is considerably larger than for nickel. The calculation using the set II radii are in support of the experimental observations. The calculated **g** tensor is anisotropic in the same manner as found for the nickel system ($g_x = 2.007$, $g_y = 2.021$, $g_z = 2.004$), with the principal anisotropy again less than that observed.

This decrease in g tensor anisotropy relative to the nickel system is directly related to the population of the palladium d orbitals, which is significantly less (0.131 Ni vs. 0.042 Pd) and the decrease in metal character of the occupied levels (e.g., $8a_g$, Ni (d) 0.914 vs. Pd (d) 0.571). The population of the 1-carbon atom however is slightly increased for the palladium SOMO (Ni 0.154 vs. Pd 0.173) in agreement with the slightly increased proton–electron coupling observed in this molecule.

Conclusion

The results of the present ESR and theoretical study strongly support the conclusions of recent electrochemical studies[8] concerning the ligand-centered nature of the one-electron reduction of the planar bis(dithio β-diketonato)nickel(II) complexes. This contrasts with the results of previous studies of the corresponding dithiocarbamate and maleonitriledithiolate complexes, where the reduction was found to be essentially metal based.[1-3] A possible

Table VI. SW-Xα Orbital Energies and Populations for the $[Pd(S_2C_3H_3)_2]^-$ $3b_{2g}$ SOMO[a]

orbital	energy[b]	populations[d]
$6b_{1g}$	−0.2485	0.505 Pd (d) + 0.009 S (s) + 0.103 S (p)
$2a_u$	−0.3133	0.071 S (p) + 0.179 Cl (p)
$3b_{2g}$[c]	−0.3127	0.042 Pd (d) + 0.067 S (p) + 0.173 Cl (p)
$3b_{3g}$	−0.4671	0.252 Pd (d) + 0.143 S (p) + 0.082 C2 (p)
$8a_g$	−0.5345	0.149 Pd (s) + 0.571 Pd (d) + 0.062 S (p)
$5b_{3u}$	−0.5349	0.111 Pd (p) + 0.209 S (p) + 0.005 C2 (s)
$2b_{1u}$	−0.5402	0.041 Pd (p) + 0.157 S (p) + 0.016 Cl (p) + 0.133 C2 (p)
$2b_{2g}$	−0.5444	0.478 Pd (d) + 0.070 S (p) + 0.061 Cl (p)
$7a_g$	−0.5854	0.038 Pd (s) + 0.885 Pd (d) + 0.006 S (p) + 0.008 C2 (p)
$1a_u$	−0.6064	0.182 S (p) + 0.068 C (p)
$6b_{2u}$	−0.6202	0.149 Pd (p) + 0.200 S (p)
$2b_{3g}$	−0.6373	0.630 Pd (d) + 0.015 S (p) + 0.032 Cl (p) + 0.090 C2 (p)
$1b_{2g}$	−0.6889	0.504 Pd (d) + 0.106 S (p) + 0.018 Cl (p)
$5b_{1g}$	−0.6893	0.310 Pd (d) + 0.017 S (s) + 0.134 S (p) + 0.012 Cl (p)
$6a_g$	−0.737	0.051 Pd (s) + 0.386 Pd (d) + 0.124 S (p)

[a] Radii set II. [b] Rydberg units. [c] Highest occupied molecular orbital. [d] Populations less than 0.005 omitted.

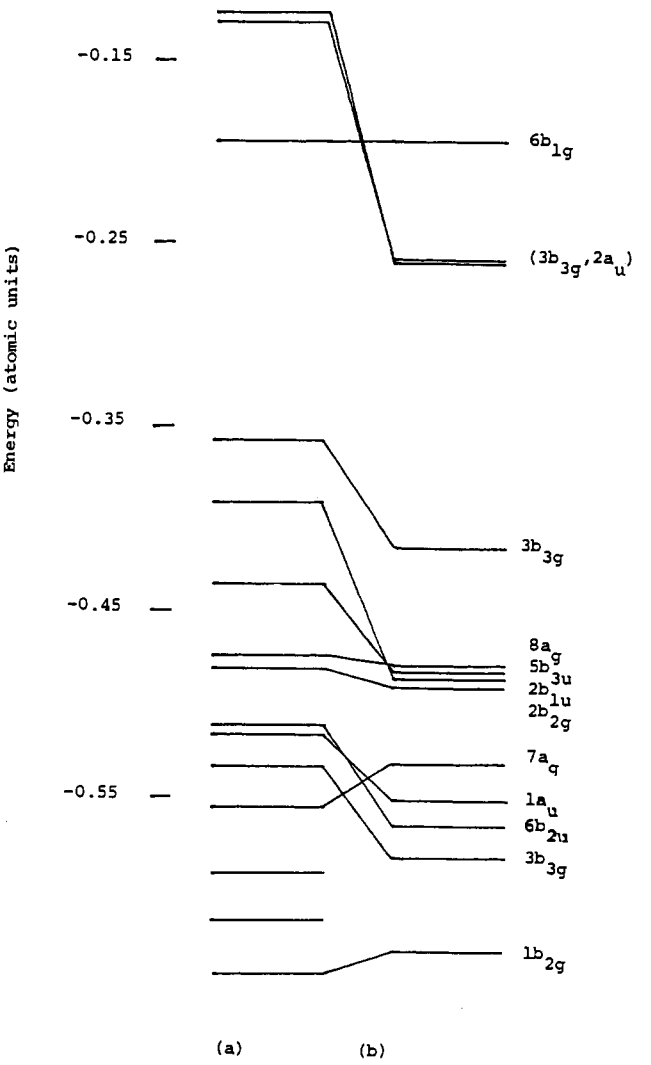

Figure 11. SW-Xα orbital energies for $[Pd(S_2C_3H_3)_2]^-$: (a) calculation I; (b) calculation II.

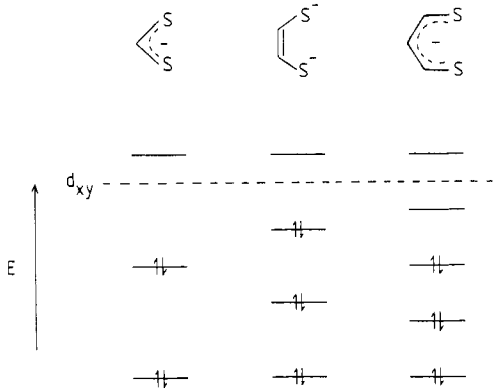

Figure 12. Qualitative π-molecular orbital energy level diagram for 1,1-, 1,2-, and 1,3-dithio ligands.

reason for this can be seen from a qualitative π-molecular orbital energy level diagram for the ligands (Figure 12). The increasing degree of conjugation from the 1,1- to the 1,3-dithiolate ligand results in a lowering in energy of the π-antibonding orbitals to the point where one of these becomes more stable than the lowest energy σ-antibonding metal orbital involving the d_{xy} orbital. It is interesting to note that essentially the same diagram as Figure 12 was used by Schrauzer to account for the observation that a range of oxidation states are accessible for complexes of "even" (1,2-dithio) ligands, but not for complexes of "odd" (1,1- or 1,3-dithio) ligands.[30] This argument applies only to oxidation reactions of complexes of the ligands in the oxidation states shown in Figure 12, however. It is now clear that one-electron-reduction reactions are possible in all three cases, but only in the case of the 1,3-dithio ligand do the π-orbital energies become low enough to allow ligand-centered (rather than metal-centered) reductions to take place.

One as yet unexplained feature of this model in relation to the complexes studied in the present work is that it does not seem to apply to mixed-ligand complexes such as $[Ni(SacSac)(dpe)]^+$, whose one-electron reduction is found to be essentially metal based. The possibility that additional stabilization of the ligand π orbitals in $Ni(SacSac)_2$ occurs through interaction between orbitals on the different ligands can be ruled out because the π orbitals of the complex all occur as near-degenerate pairs. Thus, there must be a lowering of the energy of the metal d orbitals in $[Ni(SacSac)(dpe)]^+$ relative to $Ni(SacSac)_2$, although the reason for this is not clear at present.

The stabilization of the (a_u, b_{2g}) ligand antibonding π orbitals relative to 1,1- and 1,2-dithio ligand complexes may be understood in terms of the stabilizing π-bonding interaction between the sulfur ligand atom and the ajacent carbon atom and the weaker antibonding interaction between these carbon-sulfur π-bonding orbitals due to the presence of the extra methene carbon in the 1,3 ligand (Figure 7). In the case of the 1,2 ligand these orbitals are raised in energy due to the stronger antibonding interaction between the adjacent 1,2-carbon atoms.[27]

Acknowledgment. We thank Janet Hope for some preliminary experiments on $Ni(SacSac)_2$ and Professor R. L. Martin for his interest in this problem. We also thank Dr. Michael Cook for a copy of the Xα-SW programs used in this study.

Registry No. $[Ni(SacSac)_2]$, 64705-81-3; $[Ni(t\text{-}BuSac\text{-}t\text{-}BuSac)_2]^-$, 61024-06-4; $[Ni(CH_2{=}CHCH_2SacSac)_2]^-$, 93304-99-5; $[Ni(CF_3SacSac)_2]^-$, 93280-88-7; $[Ni(NorSacSac)_2]^-$, 93280-89-8; $[Pd(SacSac)_2]^-$, 93280-90-1; Ni(SacSac)(dpe), 93280-91-2; Ni(*t*-BuSac-*t*-BuSac)(dpe), 93280-92-3.

(30) Schrauzer, G. N. *Acc. Chem. Res.* **1969**, *2*, 72.

Contribution from the Centre de Recherches Nucléaires, 67037 Strasbourg Cedex, France, Institut für Anorganische Chemie der Universität, Karlsruhe, Federal Republic of Germany, and Kamerlingh Onnes Laboratorium, Rijks Universiteit, Leiden, The Netherlands

Structural, Magnetic, and Electronic Properties of Europium Dihalides, EuX_2 (X = Cl, Br, I)

J. P. SANCHEZ,*† J. M. FRIEDT,† H. BÄRNIGHAUSEN,‡ and A. J. VAN DUYNEVELDT§

Received March 15, 1984

Structural, magnetic, and ^{151}Eu Mössbauer hyperfine interaction data are reported for the europium dihalides $EuCl_2$, $EuBr_2$, and EuI_2. The linear correlation observed between the isomer shift and the saturation hyperfine field indicates changing bonding ionicity, with the determinant result of increasing 6s charge and spin density with decreasing ionicity. The electronic structure and magnetic superexchange mechanisms in the dihalides are discussed and compared to those in other Eu^{2+} compounds.

Introduction

Considerable effort has been devoted over the last decade to the elucidation of the electronic and magnetic properties of divalent europium insulators or semiconductors, in particular from the hyperfine interaction parameters.[1] Most of this activity dealt with the europium monochalcogenides, with emphasis on the ferromagnetic semiconductors EuO and EuS, which are model systems for the Heisenberg exchange interactions.[2] The magnetic exchange mechanism in these materials has been analyzed thoroughly by Kasuya:[3] direct overlap and mixing of 4f and 5d orbitals between nearest-neighbor Eu^{2+} ions (nn) allows for a ferromagnetic nn exchange (J_1) whereas superexchange via anion p orbitals provides a mostly antiferromagnetic next-nearest-neighbor (nnn) coupling (J_2).

The Mössbauer isomer shift (δ_{IS}) measures the charge density at the nucleus whereas the hyperfine field (H_{hf}) reflects the spin density. Hence, if these two parameters originate from the same electrons, a linear correlation between δ_{IS} and H_{hf} is predictable in a series of chemically comparable compounds. A monotonous correlation has indeed been reported in several intermetallic alloys and is understandable under the condition of a conduction band of predominantly s character.[4,5] It is of particular interest to check

† Centre de Recherches Nucléaires.
‡ Universität Karlsruhe.
§ Rijks Universiteit.

(1) Bauminger, E. R.; Kalvius, G. M.; Nowik, I. In "Mössbauer Isomer Shifts"; Shenoy, G. K., Wagner, F. E., Eds.; North-Holland Publishing Co.: Amsterdam, 1978; Chapter 10, p 663.
(2) For recent reviews see: Wachter, P. In "Handbook on the Physics and Chemistry of Rare Earths"; Gschneidner, K. A., Jr.; Eyring, L., Eds.; North-Holland Publishing Co.: Amsterdam, 1979; Vol. II, Chapter 19, p 507. Holtzberg, F.; von Molnar, S.; Coey, J. M. D. In "Handbook of Semiconductors"; Keller, S. P., Ed.; North-Holland Publishing Co.: Amsterdam, 1980; Vol. III, p 803.
(3) Kasuya, T. *IBM J. Res. Dev.* **1970**, *14*, 214.
(4) Nowik, I.; Dunlap, B. D.; Wernick, J. H. *Phys. Rev. B: Solid State* **1973**, *8*, 238.

0020-1669/85/1324-0408$01.50/0